Modelling the capacitance of d.c. etched aluminium electrolytic capacitor foil

D. G. W. GOAD[1] and H. UCHI[2]

[1]*Boundary Technologies, 366 Lexington Drive, Buffalo Grove, IL 60089, USA;* [2]*KDK Corporation, 363, Arakawa, Takahagi-shi, Ibaraki-ken, 318 Japan*

Abstract

A model for the capacitance of anode foil used in aluminium electrolytic capacitors is compared with experimental data for commercial foils from two different manufacturers. These foils are obtained by anodic electrochemical etching to produce a porous tunnel etched structure, followed by formation of a layer of dielectric aluminium oxide in the pores. Data for the density and size of tunnels is obtained by sectioning the foil parallel to its surface with an ultramicrotome to several depths. In this paper the internal structure is modelled as a spatially random collection of hollow dielectric cylinders. Comparison of the measured capacitance with that calculated from the dimensional data and the model are in good agreement. The model predicts optimum values for tunnel size and density as a function of oxide thickness.

1. Introduction

Aluminium electrolytic capacitors are widely used in all types of electronic equipment. The capacitor consists of an anode foil on which an oxide is formed appropriate to the voltage required for operation, a suitable electrolyte and a cathode foil. The capacitance of the cathode foil is much higher than the anode foil so that the applied voltage appears mostly on the anode foil. More detailed consideration of capacitor design principles is given in [1]. In this work we are concerned exclusively with the anode foil.

In principle, a high capacitance device requires a high surface area coated with a suitable dielectric material. For aluminium electrolytic capacitors the high surface area is obtained by electrochemical etching. The dielectric coating of aluminium oxide is grown directly on this surface by a boiling water treatment followed by anodizing, a procedure termed 'formation'. Either alternating (a.c.) or direct current (d.c.) may be used for etching, depending on the intended working voltage for the device. The oxide thickness obtained in formation is proportional to the voltage (V_f) used to form the oxide during anodizing. About 1 nm of oxide is obtained per volt. During the anodizing step, the film grows by ion transport. The working voltage of the capacitor in operation must be sufficiently lower than the formation voltage so that negligible film growth occurs in use.

For applications which require a formation voltage of less than about 200 V, a.c. etching is preferred. In that case the etching is in the form of attached cubic pits with typical dimension 0.1 μm [2]. For higher working voltage use, d.c. anodic etching is used. Then the etching morphology takes the form of tunnels with diameters in the range from about one half to several micrometres. This is the type of etching used for the capacitor foil considered in this paper. It is customary to refer to foils with formation voltage in the range 200–400 V as medium voltage foils, and those with a greater formation voltage as high voltage foils.

The focus of this paper rests on the properties of the capacitor foil, therefore only a brief description of the processing steps will be given. These vary between manufacturers and full details are not available. Typically, the etching step is done in a hot chloride solution at temperatures above 70 °C. Sulfuric acid is also a common component of the etchant as it reduces the tunnel diameter [3, 4]. In the initial attack crystallographic cubic etch pits form. The pit has a fairly well defined half cubic shape [5]. Since the pit walls grow in five directions simultaneously, the depth of the pit is half the width at the surface. When the pit width increases to about 1 μm, there is a change in growth morphology, so that tunnels form from the existing pits and grow along [1 0 0] directions [6]. In the manufacture of capacitor foil for d.c. etching the metallurgical processing conditions are adjusted to produce a high degree of the preferred orientation for etching ('high cubicity' foil). During etching, aluminium dissolution occurs at the tips of active tunnels; the tunnel sidewalls become passive. The tunnel cross sections are square in shape and with diameters in the submicrometre to micrometre range. The density of the tunnels is usually $> 10^7$ per cm^2. Depending on the solution and temperature, tunnels may be grown up to about 100 μm in length. In previous

experimental work it was found that the tunnels have a significant needle-like taper [4]. A second chemical or electrochemical treatment in hot nitric acid [7] is usually applied. This has the effect of reducing the taper and making the tunnel cross section almost circular. This material is what is usually referred to as 'etched foil'.

Finally, dielectric aluminium oxide is formed in the internal pores. In principle this is simply the creation of a coherent, aluminium oxide film which is relatively free of defects. Procedural details may differ between manufacturers and are somewhat proprietary. Typically, an initial treatment in boiling water for several minutes is followed by anodic oxidation in ammonium borate solution at a current density of about $25 \, \text{mA cm}^{-2}$ at $95 \, ^\circ\text{C}$. When the potential drop across the foil reaches the formation voltage, the foil is held at this constant voltage for a total time of 10 min. At this stage the oxide may contain cracks, pores and other defects. To heal these defects, a rapid heating may be used to open the structure, and a final anodic oxidation is then applied. More details of these procedures are given in [8].

The resulting capacitance depends on the length, width, and spatial distribution of the etch tunnels, and on the subsequent anodic formation treatment. Here, these factors are discussed quantitatively as follows. The capacitance of an isolated tunnel is modelled as a cylinder of hollow dielectric. The capacitance of an array of such tunnels, with no overlapping cylinders would be the sum of all the individual tunnel capacitances, as the tunnels are parallel [9]. However, the tunnels are not normally in a geometrically regular arrangement, so the total internal surface area of the array of tunnels is reduced because some tunnels overlap. If the spatial distribution is assumed to be random (Poisson), then the consequences of the overlap can be quantified and the resulting capacitance can be modelled [10]. This allows prediction of the dependence on etching and formation parameters to be made.

Development of aluminium electrolytic capacitors has been largely empirical. In this work, the capacitance of commercial foils is measured for a range of formation voltages and compared with calculated values from the random distribution model. If the model is in reasonable agreement with measured values then it could be a useful design tool.

2. Experimental details

All foils used had a purity $>99.99\%$. A typical composition contained the following levels of impurities: Fe 8, Si 7, Cu 50 and Pb 0.5 ppm. For SEM examination of etched foils that had not been formed (Tokyo Aluminium Corporation, Japan), an oxide replica was made. A thin oxide was first formed on the internal surfaces by anodizing (to 40 V) in a $0.8 \, \text{M}$ ammonium adipate solution at room temperature. The current

density was $0.5 \, \text{mA cm}^{-2}$ until 40 V was reached, and the foil was then held at 40 V for a further 5 min. This produced a film about 40 nm thick. Aluminium was dissolved from the formed foils by immersion in a bromine–methanol solution. Finally a thin coating of gold was sputter deposited on the replica for examination in the SEM (Hitachi 2300). Commercial formed foils for 300 V use were also examined in the SEM. In this case the initial anodizing step was omitted.

Tunnel density and size measurements were made by cutting parallel to the surface of etched foils using an ultramicrotome (RMC model 6000) with a diamond knife, and examining the surface at various depths in the SEM [11, 12]. Data for etch tunnel radius and the fraction of the area etched were obtained using image analysis (Optimas).

Capacitance measurements were made at 120 Hz in a one litre beaker using a solution of $80 \, \text{g dm}^{-3}$ ammonium pentaborate at $30 \, ^\circ\text{C}$. Two sided specimens with a total area of $10 \, \text{cm}^2$ were used ($5 \, \text{cm}^2$ on each side). The counterelectrode was a large cylindrical Pt sheet. with a capacitance $>40 \, 000 \, \mu\text{F}$ [8]. This procedure is in accordance with Japan Industrial Standard EIAV RC-2364. Capacitance results are reported here per cm^2 of one side.

3. Model

Several relationships are required to estimate the capacitance of etched foil. In addition to the capacitance of a collection of randomly dispersed cylinders, the relationship between the tunnel dimensions before and after formation of the oxide dielectric is required. It is also useful to relate the observed fraction of the foil that is etched at a particular depth (the 'etch fraction') to the tunnel density and radius.

3.1. Capacitance of a cylinder

For a single tunnel the capacitance C_{tun} is given by the classical expression [13]

$$C_{\text{tun}} = \frac{2\pi\varepsilon_0\varepsilon\lambda}{\ln(R_2/R_1)} \tag{1}$$

where ε_0 is the permittivity of free space, ε is the dielectric constant and λ the tunnel length. R_1, R_2 are the inner and outer tunnel radius, after formation, as shown in Figure 1. The capacitance is proportional to the tunnel length. If the film thickness $d = R_2 - R_1$ is small compared to the radius R_1 then Equation 1 reduces to the expression for a parallel plate capacitor, $\varepsilon_0\varepsilon A/d$, where A is the internal area $2\pi R_1\lambda$ of a single tunnel.

3.2. Capacitance of a collection of tunnels

For a collection of tunnels with a density $N \, \text{cm}^{-2}$, the capacitance per cm^2 is less than N times the capacitance
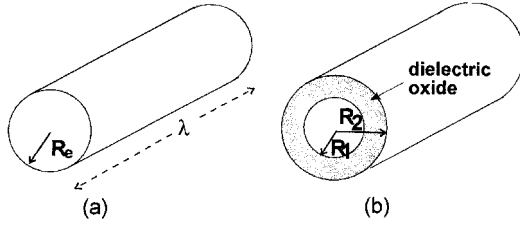
Fig. 1. Schematic of tunnels before (a) and (b) after formation. R_e is the radius of the etched tunnel; R_1 and R_2 are the inner and outer radius after oxide formation.

of a single tunnel because of overlap. As shown in Figure 2, only the gray nonoverlapping portion of the dielectric contributes to the capacitance.

For a Poisson (random) spatial distribution of the centres of the cylinders it is shown in reference [10] that the resulting capacitance is less than N times the capacitance of a single cylinder by the factor F where

$$F = \exp\left(-N\pi R_2^2\right) \qquad (2)$$

F is the average fraction of a tunnel that remains without overlap. Multiplying the product of Equations 1 and 2 by N, the total capacitance per cm^2, C, is given by

$$C = \frac{2\pi\varepsilon_0\varepsilon N\lambda\,\exp\left(-N\pi R_2^2\right)}{\ln(R_2/R_1)} \qquad (3)$$

3.3. *Etched and formed tunnel dimensions*

With reference to Figure 1, we need to relate the inner (R_1) and outer (R_2) radii of the tunnel after formation to the radius after etching (R_e). Normally, the thickness d of the formed layer will be proportional to the formation voltage V_f, so

$$d = R_2 - R_1 = k_1 V_f \qquad (4)$$

where k_1 is the formation constant (about 1 nm V^{-1} [14]). Assuming 100% efficiency for conversion of metal, the mass of the aluminium consumed in the formation is equal to the mass of the aluminium present as oxide in the formed film. This leads to equation (5).

$$\alpha(R_2^2 - R_e^2) = R_2^2 - R_1^2 \qquad (5)$$

where

$$\alpha = k_2\rho_{A1}/\rho_{ox} \qquad (6)$$

and α is the volume of oxide produced per volume of metal consumed, k_2 is the ratio of the mass of oxide produced to metal consumed, and ρ_{Al} and ρ_{ox} are the density of metal and oxide. Equation 5 implies a critical minimum radius for the etched tunnel. If the tunnel radius is too small it will be entirely filled during formation. This occurs when R_1 is zero; the critical value for R_e is given by Equation 7:

$$(R_e)_{crit} = d\sqrt{1 - (1/\alpha)} \qquad (7)$$

3.4. *Tunnel density and etched fraction*

In principle it is possible to measure a tunnel density, N, by direct counting using image analysis. It is, however, more convenient to measure the mean size of nonoverlapping tunnels and the fraction f of the area that is etched, and then calculate the corresponding tunnel density. To relate these quantities, we consider the probability that some random location 'P' will not be etched. The tunnel cross section is approximately circular with radius R_e. Figure 3 shows several circles with radius R_e near P. P will not be etched if no portion of a circular etch tunnel touches P. Geometrically, there must be no circles whose centres lie within a circle radius R_e centred on P. If the tunnel centres are randomly distributed, then the expectation value μ for the number of tunnels with centres in any area A is just the area times the number of tunnels per unit area (i.e. $\mu = NA$). Here the area A is πR_e^2 so $\mu = N\pi R_e^2$. Then according to the Poisson distribution [15], the probability $P(n)$ of $0, 1, 2, \ldots, n$ tunnels being present in the area A, when the expectation value is μ, is given by $\exp\left(-\mu\right)\mu^n/n!$. To calculate the probability that P is not etched, we need $P(0)$, the probability that no tunnels are centred in A. With $\mu = N\pi R_e^2$, $P(0) = \exp\left(-N\pi R_e^2\right)$, and the etched fraction f is given by

$$f = 1 - P(0) = 1 - \exp\left(-N\pi R_e^2\right) \qquad (8)$$

Rearranging Equation (8) we obtain an expression for the tunnel density in terms of f and R_e.

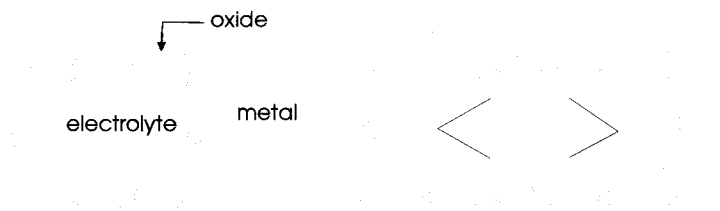$$N = \frac{-\ln(1-f)}{\pi R_e^2} \qquad (9)$$

Fig. 2. Cross section of overlapping tunnels (only the gray portion of the oxide contributes to the capacitance).
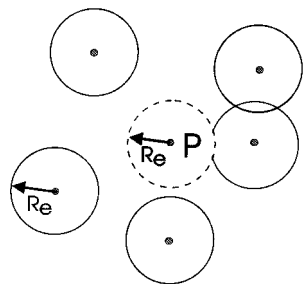
Fig. 3. Schematic of overlapping tunnels for calculation of relationship of etched area, tunnel size and density.

4. Results and discussion

The appearance of an oxide replica at a relatively early stage of the etch is shown in Figure 4. There is some tendency of the tunnels to cluster around surface topographical features such as rolling lines.

Figure 5 shows the appearance of a cross section of a foil formed to 300 V. The edges of some tunnels are broken, allowing the interior shape of the tunnels and the oxide to be seen. A common feature of the etch tunnel distribution is the accumulation of a large number of pits or tunnels within the first 10 μm of the surface. In addition, many tunnels change direction near the surface.

Direct measurement of the positions of tunnel centres was done for one sample at a depth of 20 μm over an area 30 μm×30 μm. The area was subdivided into 25 equal areas. The mean and variance of the number of tunnels in each area was 9.0 and 8.5. This is consistent with a Poisson distribution, for which the mean and variance are equal [15].

Figure 6 shows capacitance data for 4 different foils from two manufacturers (identified as A and B). A1 and B1 are medium voltage foils intended for formation voltages of 200–400 V; A2 and B2 are high voltage foils for >400 V. The figure shows how the capacitance per cm^2 varies with the formation voltage.

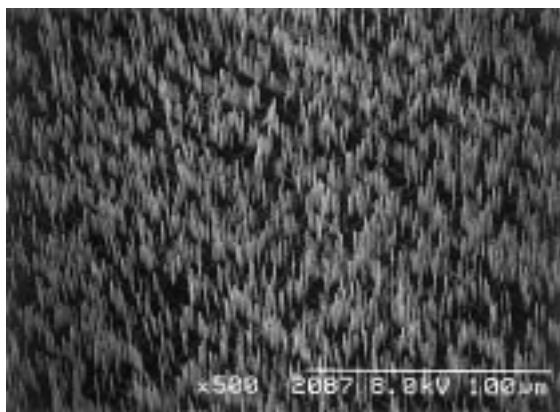Tunnel density and dimensional data were obtained for one of these foils (A1) using the ultramicrotome

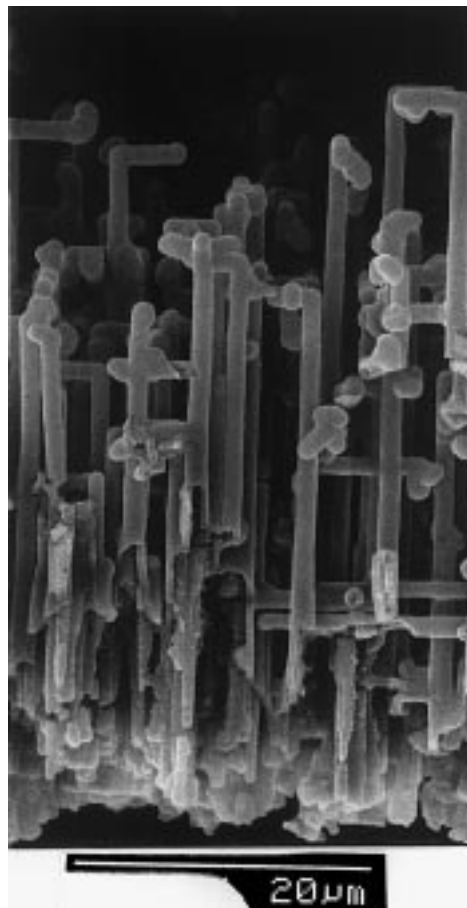Fig. 5. Cross section of commercial foil formed to 300 V.

technique. SEM micrographs of the unformed foil was obtained for depths from 0 to 40 μm. Data for etch tunnel radius and the fraction of the area etched are shown in Table 1. Tunnel densities are calculated as described previously using Equation 9. As there is a significant variation in tunnel radius and density with depth, the tunnels cannot be characterized by single values for these two quantities. Mean values of tunnel density and radii are used for five sections of 10 μm thickness (i.e. for the 20–30 μm section, the mean of the values determined at 20 and 30 μm is used). The tunnel density at 50 μm is zero. For each 10 μm thick section Equations 4 and 5 are used to determine the inner and outer tunnel radii after formation, and Equation 3 allows the capacitance to be calculated at any formation voltage, using the values for constants shown in Table 2. Finally the total capacitance at any voltage is obtained by adding the contribution for the five sections. Figure 7 shows a comparison of experimental and calculated data.

The observed values average about 95% of the calculated values, in the range 91–100% of those observed. No attempt was made to vary the parameters in Table 2 to improve the fit. This agreement of the observed and calculated values is within the accuracy of the measurements and the precision of the model
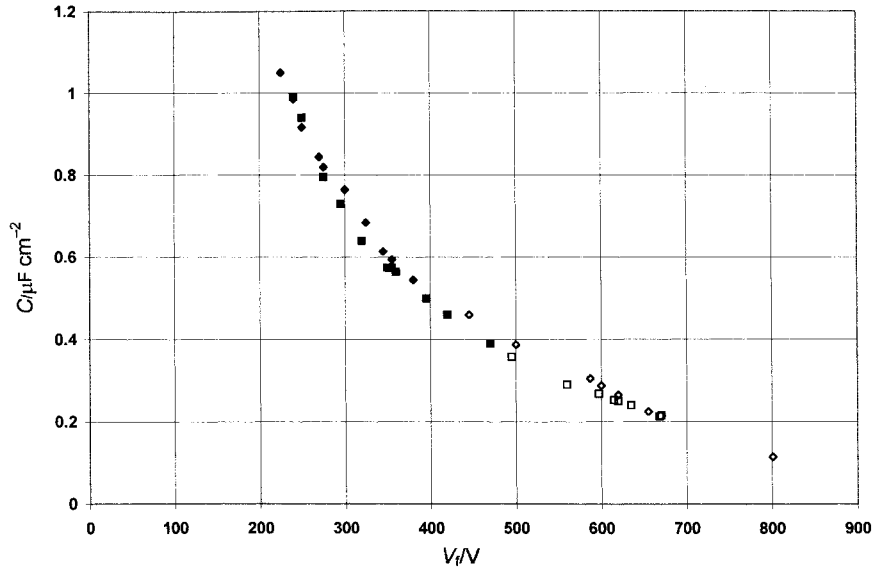

Fig. 4. Replica of surface after 10 s etch in etchant 1 N HCl, 7 N H$_2$SO$_4$ + 10 g dm^{-3} aluminium; 200 mA cm^{-2} and 77 °C; pretreatment: 40 s immersion in 0.1 M HF at 40 °C.

Fig. 6. Capacitance per cm² and formation voltage for four foils. A and B refer to manufacturers, 1 and 2 are intended for medium (200–400) and high (>400) V use respectively. Key: (◆) A1, (◇)A2, (■) B1 and (□) B2.

Table 1. Tunnel size data for foil (A1) from microtome measurements

Depth /μm	Radius /μm	Area fraction etched	10^{-7}(tunnel density) /cm²
0	0.48	0.75	19.6
10	0.44	0.23	4.4
20	0.40	0.20	4.4
30	0.35	0.195	5.6
40	0.36	0.08	2.1

Table 2. Values used in capacitance calculation

Quantity	Symbol	Value	Units
Dielectric constant	ε	8.5	none
Formation constant	k_1	0.001	μV^{-1}
Volume oxide: volume metal	α	1.84	none

parameters. The form of the curve and the actual values are in good agreement with experiment.

The critical minimum values for the etch tunnels radius, from Equation 7, are 0.11 and 0.22 μm at formation voltages of 200 and 400 V, respectively. This may be compared to the observed radius (averaged over the depth) of 0.41 μm for this foil.

4.1. *Optimization of tunnel parameters*

The conditions that maximize the capacitance may be obtained by setting the derivative of C with respect to tunnel density and radius R_2 equal to zero. The first condition leads to
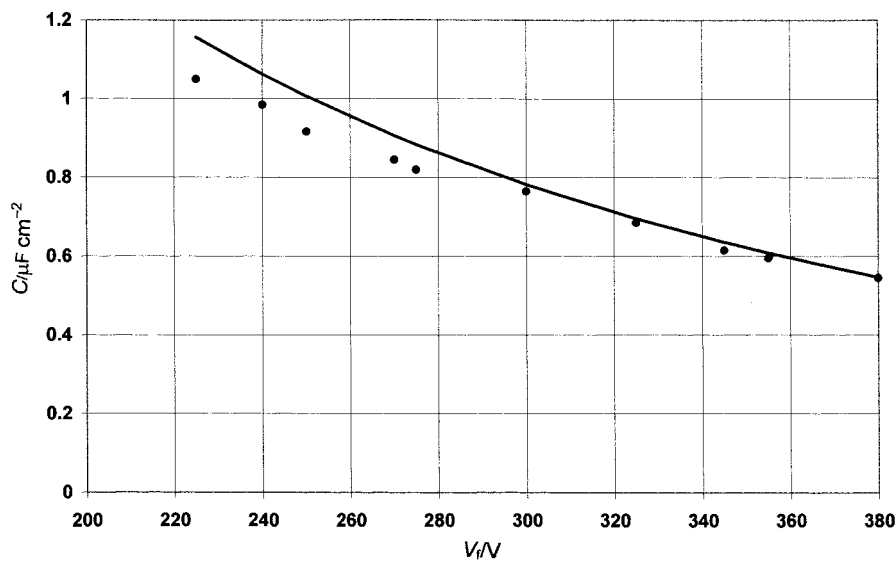
$$N\pi R_2^2 = 1 \tag{10}$$

Fig. 7. Capacitance for foil (A1). Key: (●) observed; (——) calculated.

and the second to

$$2N\pi R_2^2 \frac{R_2 - d}{d} \ln \frac{R_2}{R_2 - d} = 1 \tag{11}$$

On substituting Equation 10 in Equation 11 we find a numerical solution $R_2 = 1.398d$.

Calculated optimum tunnel density and radii for several formation voltages are shown in Table 3. The maximum values of the capacitance, C_{max}, may be obtained by substitution in Equation 3. Then,

$$C_{max} = \frac{k_3 \lambda}{k_1^2 V_f^2} \tag{11}$$

where

$$k_3 = \frac{2\varepsilon_0\varepsilon}{(1.398)^2 \ln(1.398/0.398)e} \tag{12}$$

k_3 has the numerical value $2.25 \times 10^{-7} \, \mu\text{F cm}^{-1}$. The maximum energy density on charging to V_f is $C_{max}V_f^2/2\lambda$. From Equation 11 this is $k_3/2k_1^2$, which depends only on the oxide properties and is independent of the formation voltage. The maximum capacitance in $\mu\text{F cm}^{-2}$ may be conveniently estimated as $2.25 \times 10^3 \times$ (mean tunnel length μm^{-1})/(formation voltage V^{-1})^2.

The optimum capacitance values suggested by the model (for 50 μm tunnels) are shown in Figure 8 along with actual values from commercial foils. It is clear that at the higher voltages, capacitance values obtained approach 100% of the theoretical maximum, as the optimal tunnel densities and dimensions suggested in Table 3 are readily achieved. At lower voltages, the suggested tunnel radii are smaller than those obtained in commercial practice. It is difficult to make tunnels with radii $<0.5 \, \mu$m and lengths 40 μm or more. For formation voltages below about 200 V, a.c. etching is preferred, because the dimensions of the characteristic half

Table 3. Calculated optimum parameters

Formation voltage, V_f /V	Formed radius, R_2 /μm	Etched radius, R_e /μm	Tunnel density $\times 10^{-7}$ /cm^2
200	0.28	0.17	41.0
400	0.56	0.33	10.2
600	0.84	0.50	0.45
800	1.12	0.66	0.25

cube geometry can be much smaller ($\sim 0.1 \, \mu$m) than the smallest obtainable tunnel diameter [2].

4.2. *Limitations of the model*

The assumption of the randomness of the distribution of tunnel centres is a paradigm from which some deviation may be expected. The real spatial distribution on the surface in the early stages of etching is usually not random, and tends to cluster around surface topographical features such as rolling lines, as shown in Figure 1. A deviation from randomness of a different kind may be expected in the later stages of the etch, when a significant fraction of the surface is already etched. It would seem that the centers of new surface pits must originate in the remaining unetched surface. This effect would tend to make the internal area greater than that of a strictly random arrangement, increasing the capacitance.

In this model the distribution of tunnel radii was not taken into account; the tunnels are assumed to have the same diameter. Tunnels with radius less than the critical radius will be entirely filled with oxide after formation and will not contribute to capacitance. This effect would reduce the capacitance. However, this would not be expected to be significant with the foil (A1) for which tunnel size data were obtained. In that case the critical radius varies from about 25 to 50% of the observed mean value. It is estimated that at most a few per cent of
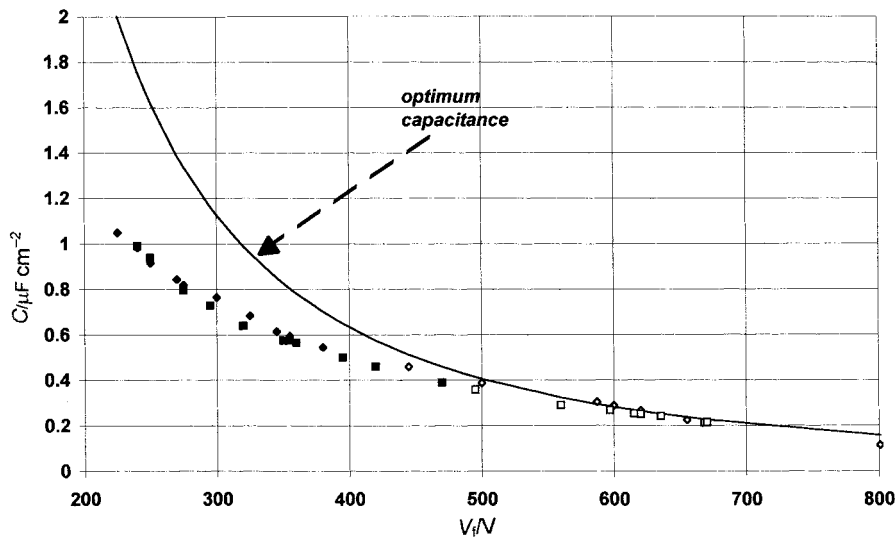

Fig. 8. Comparison of actual capacitances and optimized values according to the model. Key: (◆) A1, (◇) A2, (■) B1 and (□) B2.

tunnels would be this small. The possible influence of tunnels which are parallel to the surface or which branch was also not considered. In view of the difficulty of obtaining accurate distribution data, and the good fit of the model, such refinements did not seem warranted.

5. Conclusions

A model for tunnel distribution in which the tunnels are randomly distributed over the surface was investigated. Measured and calculated capacitances from the model are in good agreement. For formation voltages greater than 500 V, measured capacitances are at least 90% of the optimum value. With lower formation voltages a smaller fraction of the optimized values is obtained; for example, using a 200 V formation the experimental capacitance value obtained is about 50% of the optimized value. The problem in obtaining optimized capacitances at lower formation voltages is due to the small diameter of the tunnels required, which is difficult to realize in practice.

Acknowledgements

References

1. A.R. Morley and D.S. Campbell, *Radio Electron. Eng.* **43** (1973) 421.
2. C.K. Dyer and R.S. Alwitt, *J. Electrochem. Soc.* **128** (1981) 300.
3. H. Uchi, R. Yonemori, H. Sugiyama and A. Yamada, *Japan J. Technol. Educ.* **2** (1993) 33.
4. D. Goad, *J. Electrochem. Soc.* **144** (1997) 1965.
5. B.J. Wiersma and K.R. Hebert, *J. Electrochem. Soc.* **138** (1991) 48.
6. R.S. Alwitt, H. Uchi, T.R. Beck and R.C. Alkire, *J. Electrochem. Soc.* **131** (1984) 13.
7. A. Kioke, H. Fujiwara and M. Manabu, *Japanese patent 2 303 018* (1990).
8. KDK Corporation, Tokyo, Japan, Catalog EF-153, section 11, test methods (1996).
9. C.G. Dunn, R.B. Bolon, A.S. Alwan and A.W. Stirling, *J. Electrochem. Soc.* **118** (1971) 381.
10. L.A. Kostelova, R.A. Mirziev, I.T. Rosin and E.V. Kharitonov, *Elektrokhimiya* **15** (1979) 648.
11. K. Shimizu, G.M. Brown, K. Kobayashi, P. Skeldon, G.E. Thompson and G.C. Wood, *ATB Metallurgie* **27** (1997) 188.
12. N. Reid and J.E. Beesley, 'Sectioning and Cryosectioning for Electron Microscopy', (Elsevier, Oxford, 1991).
13. D. Halliday and R. Resnick, 'Physics', 2nd edn, (J. Wiley & Sons, New York, 1966), chapter 30.
14. C.K. Dyer and R.S. Alwitt, *Electrochim. Acta* **23** (1978) 347.
15. G.E.P. Box, W.G. Hunter and J.S. Hunter, *'Statistics for Experimenters'* (J. Wiley & Sons, New York, 1978).